

---

# WeightedPose: Generalizable Cross-Pose Estimation via Weighted SVD

---

Xuxin Cheng, Heng Yu, Harry Zhang, Wenxing Deng

## Abstract

We present a novel method for robotic manipulation tasks in human environments that require reasoning about the 3D geometric relationship between a pair of objects. Traditional end-to-end trained policies, which map from pixel observations to low-level robot actions, struggle to reason about complex pose relationships and have difficulty generalizing to unseen object configurations. To address these challenges, we propose a method that learns to reason about the 3D geometric relationship between objects, focusing on the relationship between key parts on one object with respect to key parts on another object. Our standalone model utilizes Weighted SVD to reason about both pose relationships between articulated parts and between free-floating objects. This approach allows the robot to understand the relationship between the oven door and the oven body, as well as the relationship between the lasagna plate and the oven, for example. By considering the 3D geometric relationship between objects, our method enables robots to perform complex manipulation tasks that reason about object-centric representations. We open source the code and demonstrate the results here <sup>1</sup>.

## 1 Introduction

Many manipulation tasks require a robot to move an object to a location relative to another object. For example, a cooking robot may need to place a lasagna in an oven, place a pot on a stove, place a plate in a microwave, place a mug onto a mug rack, or place a cup onto a shelf. Understanding and placing objects in task-specific locations is a key skill for robots operating in human environments. Further, this skill should generalize to novel objects within the training categories, such as placing new trays into the oven or new mugs onto a mug rack.

A common approach in robot learning is to train a policy "end-to-end," mapping from pixel observations to low-level robot actions. However, end-to-end trained policies cannot easily reason about complex pose relationships such as the ones described above, and they have difficulty generalizing to unseen object configurations. In contrast, we propose a method that learns to reason about the 3D geometric relationship between a pair of objects. For the type of tasks defined above, the robot needs to reason about the relationship between key parts on one object with respect to key parts on another object. Specifically, the robot needs to reason about both the relationship between the oven door and the oven body, as well as the relationship between the lasagna plate and the oven. We propose a standalone model that utilizes Weighted SVD to reason about both pose relationship between articulated parts and between free-floating objects.

## 2 Background

**Object Pose Estimation:** Pose estimation is the task of detecting and inferring the 6DoF pose of an object, which includes its position and orientation, with respect to some previously defined

---

<sup>1</sup><https://github.com/harryzhang0G/weighted-pose/tree/main>

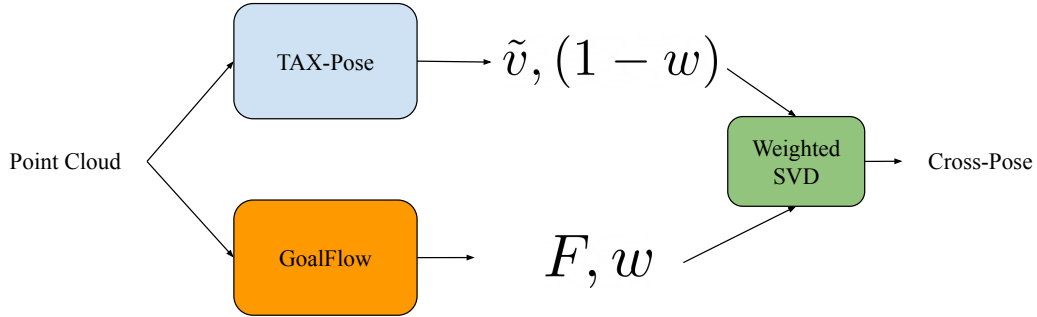


Figure 1: Unified Weighted Pose architecture. The model first takes as input a point cloud, and then learns to predict a weight for the point cloud. This weight is used in the downstream SVD module to combine the GoalFlow and TAX-Pose outputs.

object reference frame (19; 28; 36; 10; 11; 32). Recent work (20; 27; 33; 21) proposed to use 3D semantic keypoints as an alternative form of object representation. While keypoint-based methods can generalize within an object class, they require a significant amount of hand annotated data or access to a simulated version of the task to learn to estimate the keypoint locations. In contrast, our method is able to learn from just 10 real-world demonstrations. Another approach is to use dense embeddings, such as Dense Object Nets (DON) (9) and Neural Descriptor Fields (NDF) (31; 7), which achieve generalization across classes by predicting dense embeddings in the observation and matching them to embeddings of the demonstration objects. However, DON (9) and NDF (31) assume that the target object is moved relative to a static reference object in a “known canonical configuration” (e.g. the pose of the mug rack in NDF (31) is assumed to be known and fixed). In contrast, our method reasons about the geometric relationship between a pair of objects and hence does not need to assume a static environment.

**Articulated Object Manipulation:** Manipulation of articulated objects and other objects with non-rigid properties remains an open research area due to the objects’ complex geometries and kinematics. Previous work proposed manipulating such objects by hand-designed analytical methods, such as the immobilization of a chain of hinged objects by (5; 29; 1; 2; 39). Berenson et al. (3) proposed a planning framework for manipulation under kinematic constraints. Katz et al. (15) proposed a method to learn such manipulation policies in the real-world using a grounded relational representation learned through interaction. With the development of larger-scale datasets of articulated objects such as the PartNet dataset by Mo et al. (22) and Partnet-Mobility by Xiang et al. (35); Sim et al. (30); Jin et al. (14), several works have proposed learning methods based on large-scale simulation and supervised visual learning. Mo et al. (23) proposed to learn articulation manipulation policies through large-scale simulation and visual affordance learning. Xu et al. (37) proposed a system that learns articulation affordances as well as an action scoring module, which can be used to articulate objects. Several works have focused specifically on visual recognition and estimation of articulation parameters, learning to predict the pose (42; 45; 43; 38; 34; 12; 16) and identify articulation parameters (13; 41; 44) to obtain action trajectories. Moreover, (24; 4; 6; 17; 18; 8) tackle the problem using statistical motion planning.

### 3 Method

We first slightly modify the FlowBot 3D training objective. Instead of defining an instantaneous motion vector field as the training data directly, we make the network learn to output a flow field to the completely open state directly. Since this version of FlowBot 3D learns to output a dense representation to the goal state directly, we call this model Goal Flow.

Formally, given a point cloud  $\{\mathbf{p}_i\} \forall i \in \{1, \dots, N\}$  this Goal Flow model outputs a dense flow field  $F \in \mathbb{R}^{N \times 3}$ , where each flow vector  $\delta_i \in \mathbb{R}^3$  in the  $F$  represents a goal flow vector such that point  $p_i + \delta_i$  is in the fully open goal state. Ideally, this model should be deployed exclusively for articulated objects in that Goal Flow was shown to achieve suboptimal performances in (25; 26).

To combine the Goal Flow model with TAX-Pose, we also make the Goal Flow network output an auxiliary weight  $w \in \mathbb{R}$ , which assigns weight  $w$  to Goal Flow and  $1 - w$  to TAX-Pose.

For the TAX-Pose component of the Weighted Pose unified architecture, we do not make any significant modifications and ideally the TAX-Pose model should be deployed for free-floating objects exclusively.

In TAX-Pose, we have:

$$\mathcal{J}(\mathbf{T}_{AB}) = \sum_{i=1}^{N_A} \alpha_i^A \|\mathbf{T}_{AB} \mathbf{p}_i^A - \tilde{\mathbf{v}}_i^A\|_2^2 + \sum_{i=1}^{N_B} \alpha_i^B \|\mathbf{T}_{AB}^{-1} \mathbf{p}_i^B - \tilde{\mathbf{v}}_i^B\|_2^2,$$

where

$$\mathbf{A} = [\mathbf{P}_A^{*\top} \quad \tilde{\mathbf{V}}_B^{*\top}], \quad \mathbf{B} = [\tilde{\mathbf{V}}_A^{*\top} \quad \mathbf{P}_B^{*\top}]^\top, \quad \mathbf{\Gamma} = \text{diag}([\alpha_A \quad \alpha_B])$$

Now we want to add another term in the SVD step. Specifically, we want the network to learn which one of the two models, TAX-Pose and Goal-Flow, is more important based on point cloud observations. Thus, we want a SVD step that incorporates the TAX-Pose residual, weighted by  $(1 - w)$  and Goal-Flow weighted by  $w$ . So the new SVD formulation becomes:

$$\begin{aligned} \mathcal{J}(\mathbf{T}_{AB}) = (1 - w) & \left[ \sum_{i=1}^{N_A} \alpha_i^A \|\mathbf{T}_{AB} \mathbf{p}_i^A - \tilde{\mathbf{v}}_i^A\|_2^2 + \sum_{i=1}^{N_B} \alpha_i^B \|\mathbf{T}_{AB}^{-1} \mathbf{p}_i^B - \tilde{\mathbf{v}}_i^B\|_2^2 \right] \\ & + w \sum_{i=1}^{N_A} \|\mathbf{T}_{AB} \mathbf{p}_i^A - (\mathbf{p}_i^A + \delta_i^A)\|_2^2, \end{aligned}$$

where  $\delta_i^A$  is the  $i$ -th point's goal flow. To make this approach viable we optimize  $R$  and  $t$  in  $\mathbf{T}_{AB}$  separately:

$$\begin{aligned} J = & \sum_i^{N_A} ((1 - w)\alpha_i \|R\mathbf{p}_i^A + t - \tilde{\mathbf{v}}_i^A\|^2 + w\|R\mathbf{p}_i^A + t - \mathbf{p}_i^A + \delta_i^A\|^2) \\ & + \sum_i^{N_B} (1 - w)\alpha_i \|R^{-1}\mathbf{p}_i^B - t - \tilde{\mathbf{v}}_i^B\|^2 \end{aligned}$$

We first solve for the optimal translation  $t^*$ :

$$\begin{aligned}
\frac{\partial J}{\partial t} &= 0 \\
&= \sum_i^{N_A} (2(1-w)\alpha_i (t + R\mathbf{p}_i^A - \tilde{\mathbf{v}}_i^A) + 2w (t + R\mathbf{p}_i^A - \mathbf{p}_i^A - \delta_i^A)) \\
&\quad + 2(1-w) \sum_i^{N_B} \alpha_i (R^{-1}\mathbf{p}_i^B - t - \tilde{\mathbf{v}}_i^B) \\
&= \sum_i^{N_A} ((2-2w)\alpha_i + 2w) t + ((2-2w)\alpha_i + 2w) R\mathbf{p}_i^A - 2w\delta_i^A - (2-2w)\alpha_i \tilde{\mathbf{v}}_i^A - 2w\mathbf{p}_i^A \\
&\quad + \sum_i^{N_B} -(2-2w)\alpha_i t + (2-2w)\alpha_i (R^{-1}\mathbf{p}_i^B - \tilde{\mathbf{v}}_i^B) \\
&= \left[ \sum_i^{N_A} [(2-2w)\alpha_i + 2w] + \sum_i^{N_B} -(2-2w)\alpha_i \right] t \\
&\quad + \sum_i^{N_A} ((2-2w)\alpha_i + 2w) R\mathbf{p}_i^A - 2w\delta_i^A - (2-2w)\alpha_i \tilde{\mathbf{v}}_i^A - 2w\mathbf{p}_i^A \\
&\quad + \sum_i^{N_B} (2-2w)\alpha_i (R^{-1}\mathbf{p}_i^B - \tilde{\mathbf{v}}_i^B) \\
t^* &= - \left( \sum_i^{N_A} ((2-2w)\alpha_i + 2w) R\mathbf{p}_i^A - 2w\delta_i^A - (2-2w)\alpha_i \tilde{\mathbf{v}}_i^A - 2w\mathbf{p}_i^A \right. \\
&\quad \left. + \sum_i^{N_B} (2-2w)\alpha_i (R^{-1}\mathbf{p}_i^B - \tilde{\mathbf{v}}_i^B) \right) / \left[ \sum_i^{N_A} [(2-2w)\alpha_i + 2w] + \sum_i^{N_B} -(2-2w)\alpha_i \right]
\end{aligned}$$

Further simplifying, we have:

$$\begin{aligned}
t^* &= \frac{(1-w) \sum_i^{N_A} \alpha_i^A (\tilde{\mathbf{v}}_i^A - R\mathbf{p}_i^A)}{(1-w) \sum_i^{N_A} \alpha_i^A + w \sum_i^{N_A} 1 + (1-w) \sum_i^{N_B} \alpha_i^B} \\
&\quad + \frac{w \sum_i^{N_A} (\mathbf{p}_i^A + \delta_i^A) - R\mathbf{p}_i^A}{(1-w) \sum_i^{N_A} \alpha_i^A + w \sum_i^{N_A} 1 + (1-w) \sum_i^{N_B} \alpha_i^B} \\
&\quad + \frac{(1-w) \sum_i^{N_B} \alpha_i^B (\tilde{\mathbf{v}}_i^B - R^{-1}\mathbf{p}_i^B)}{(1-w) \sum_i^{N_A} \alpha_i^A + w \sum_i^{N_A} 1 + (1-w) \sum_i^{N_B} \alpha_i^B}
\end{aligned}$$

Note here that we colorcode the expression here. Intuitively, the resulting translation is a weighted sum of three translation terms. The **red** color represents the action object's translation via TAX-Pose, the **blue** color represents the action object's translation via GoalFlow, and the **purple** color represents the anchor object's translation via TAX-Pose.

We can then construct the matrices as follows:

$$\begin{aligned}
\mathbf{A} &= [\mathbf{P}_A^\top \quad \tilde{\mathbf{V}}_B^\top \quad \mathbf{P}_A^\top], \quad \mathbf{B} = [\tilde{\mathbf{V}}_A^\top \quad \mathbf{P}_B^\top \quad \mathbf{P}_A^\top + \Delta_A]^\top \\
\mathbf{\Gamma} &= \begin{bmatrix} (1-w) \cdot \alpha_A & 0 & 0 \\ 0 & (1-w) \cdot \alpha_B & 0 \\ 0 & 0 & w \end{bmatrix}
\end{aligned}$$

where  $\Delta_A$  is the de-meanded goal flow field. Note here that everything here is **NOT** de-meanded.

We then solve for the SVD:

$$\mathbf{U}\mathbf{\Sigma}\mathbf{V}^\top = \text{svd}(\mathbf{A}\mathbf{\Gamma}\mathbf{B}^\top)$$

and then we solve for rotation matrix  $R$ . Plugging it back into the  $t^*$  equations we get  $t$ .

To train the WeightedPose, we use a set of losses defined below, which are similar to those in (25). We assume we have access to a set of demonstrations of the task, in which the action and anchor objects are in the target relative pose such that  $\mathbf{T}_{AB} = \mathbf{I}$ .

**Point Displacement Loss:** Instead of directly supervising the rotation and translation (as is done in DCP), we supervise the predicted transformation using its effect on the points. For this loss, we take the point clouds of the objects in the demonstration configuration, and transform each cloud by a random transform,  $\hat{\mathbf{P}}_A = \mathbf{T}_\alpha \mathbf{P}_A$ , and  $\hat{\mathbf{P}}_B = \mathbf{T}_\beta \mathbf{P}_B$ . This would give us a ground truth transform of  $\mathbf{T}_{AB}^{GT} = \mathbf{T}_\beta \mathbf{T}_\alpha^{-1}$ ; the inverse of this transform would move object  $B$  to the correct position relative to object  $A$ . Using this ground truth transform, we compute the MSE loss between the correctly transformed points and the points transformed using our prediction.

$$\mathcal{L}_{\text{disp}} = \|\mathbf{T}_{AB} \mathbf{P}_A - \mathbf{T}_{AB}^{GT} \mathbf{P}_A\|^2 + \|\mathbf{T}_{AB}^{-1} \mathbf{P}_B - \mathbf{T}_{AB}^{GT-1} \mathbf{P}_B\|^2 \quad (1)$$

**Direct Correspondence Loss.** While the Point Displacement Loss best describes errors seen at inference time, it can lead to correspondences that are inaccurate but whose errors average to the correct pose. To improve these errors we directly supervise the learned correspondences  $\tilde{V}_A$  and  $\tilde{V}_B$ :

$$\mathcal{L}_{\text{corr}} = \|\tilde{V}_A - \mathbf{T}_{AB}^{GT} \mathbf{P}_A\|^2 + \|\tilde{V}_B - \mathbf{T}_{AB}^{GT-1} \mathbf{P}_B\|^2. \quad (2)$$

**Correspondence Consistency Loss.** Furthermore, a consistency loss can be used. This loss penalizes correspondences that deviate from the final predicted transform. A benefit of this loss is that it can help the network learn to respect the rigidity of the object, while it is still learning to accurately place the object. Note, that this is similar to the Direct Correspondence Loss, but uses the predicted transform as opposed to the ground truth one. As such, this loss requires no ground truth:

$$\mathcal{L}_{\text{cons}} = \|\tilde{V}_A - \mathbf{T}_{AB} \mathbf{P}_A\|^2 + \|\tilde{V}_B - \mathbf{T}_{AB}^{-1} \mathbf{P}_B\|^2. \quad (3)$$

**Direct SE(3) Transformation Loss.** We also define a loss directly for the transformation outputted in  $SE(3)$ , supervising between the SVD output pose and ground-truth pose.

$$\mathcal{L}_{\text{tf}} = \|\mathbf{T}_{AB} - \mathbf{T}_{AB}^{GT}\|_F \quad (4)$$

## 4 Experiments

We define a PartNet-Mobility Placement task as placing a given action object relative to an anchor object based on a semantic goal position. This would require the model to be able to output cross-pose for both the articulated parts and the free-floating objects. We select a set of household furniture objects from the PartNet-Mobility dataset (35) and a set of small rigid objects released with the Ravens simulation environment (40). When the model is required to estimate goal pose for the articulated part, following the terminology in (25), the action object would be the articulated part (e.g. doors, drawers), and the anchor object would be the static body of the furniture. In contrast, when the model is estimating goal pose for free floating objects, then it becomes the same setting as in (25). We compare the proposed method to several baselines. First, we compare against TAX-Pose trained on both free-floating and articulated objects as well as Goal-Flow trained on both categories of objects. We then compare against an oracle model that classifies if the objects of interest are free-floating or articulated, and deploys the model accordingly.

We describe the baselines in details:

- Goal Flow Pretrained (GF Pretrained): Pretrain Goal Flow on articulated objects only and test on both articulated and free-floating objects.
- TAX-Pose Pretrained (TP Pretrained): Pretrain TAX-Pose on free-floating objects only and test on both articulated and free-floating objects.
- Weighted Pose Original Loss (WP OG Loss): Weighted Pose trained and test on both free-floating and articulated objects using the original TAX-Pose loss.
- Weighted Pose Post-SVD Loss (WP Post-SVD): Weighted Pose trained and test on both free-floating and articulated objects but using the post-SVD TAX-Pose loss.

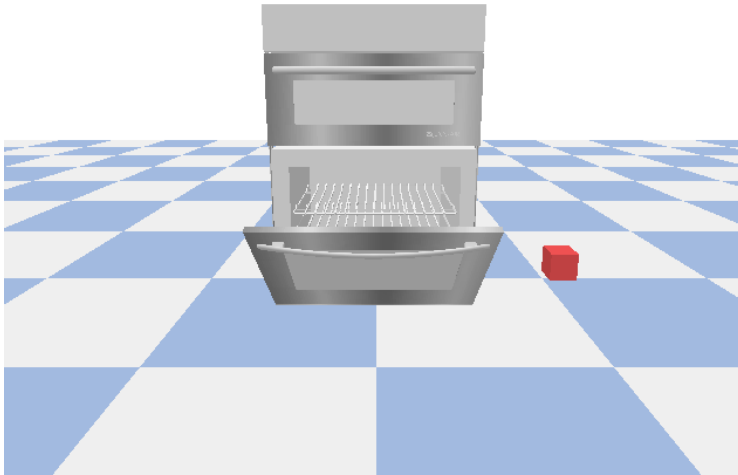


Figure 2: Task illustration. The model needs to first output goal pose for opening the oven door, and then output goal pose for putting the block inside the oven.

- **Weighted Pose Post-SVD & Transformation Loss (WP Post-SVD):** Weighted Pose trained and test on both free-floating and articulated objects but using both the post-SVD TAX-Pose loss and direct transformation loss. Where the transformation loss is the MSE between the predicted  $SE(3)$  transformation and the ground-truth  $SE(3)$  transformation.

We use the same PartNet-Mobility dataset as in TAX-Pose to evaluate the system. For semantic tasks, we will only select the “In” task as it is the most intuitive task. However, other than just performing evaluation on the free-floating objects, we will also evaluate the method on opening the articulate objects. Under this formulation, the action object is the articulated part and the anchor object is the static body. We will measure rotational error, translational error, and per-point MSE in our experiments. We follow the same train-val split as in TAX-Pose’s PartNet-Mobility dataset.

In Table 1, Goal Flow Pretrained baseline fails on free-floating objects and excels on articulated objects. Similarly for TAX-Pose pretrained, since it was trained on free-floating objects, it does do well on articulated objects, as the high rotational and translational errors indicate.

We next evaluate the variations of WeightedPose, which differ in the training paradigms. Using Weighted Pose Original Loss, which is trained using the original TAX-Pose loss, we are able to achieve better performance on both articulated and free-floating objects. Interestingly, the results we achieve using Weighted Pose Original Loss for articulated objects are better than the results from using Goal Flow pretrained on articulated objects.

While ideally, the  $w$  learned in this method should effectively act as a classifier of the input object (1 for articulated objects, 0 for free-floating objects). Intuitively, given a perfect  $w$ , the performance of WeightedPose would be upper-bounded by Goal Flow’s performance on articulated objects and by TAX-Pose on free-floating objects. However, a weighted combination of the two results due to the imperfect learned  $w$  weight could potentially correct the mistake made by each model by summing the results with a weighted sum. This may explain why WeightedPose sometimes performs better than its hypothesized upper bound on some objects.

Lastly, results suggest that the original loss used in TAX-Pose yields the best overall performance. However, it is worth noting that by using post-SVD loss during training, we are able to achieve lower translational error in test time. Interestingly, by introducing a direct  $SE(3)$  supervision, the results degrade marginally.

	Metrics	GF Pretrained		TP Pretrained		WP OG Loss		WP Post-SVD		WP Post SVD + T	
		FF	Art	FF	Art	FF	Art	FF	Art	FF	Art
Train	Rot err	31.61	<b>5.16</b>	<b>2.61</b>	55.78	11.69	3.15	13.14	3.28	14.04	5.52
	Trans err	1.21	<b>0.16</b>	<b>0.04</b>	0.98	0.14	0.08	0.21	0.07	0.21	0.07
	PP MSE	1.04	<b>0.04</b>	<b>0.01</b>	0.85	0.07	0.05	0.09	0.04	0.11	0.08
Val	Rot err	35.5	<b>9.14</b>	<b>9.87</b>	59.73	11.22	9.01	14.13	9.71	13.06	10.03
	Trans err	1.3	<b>0.19</b>	<b>0.18</b>	0.99	0.26	0.15	0.22	0.18	0.23	0.18
	PP MSE	1.07	<b>0.1</b>	<b>0.15</b>	0.82	0.16	0.11	0.17	0.12	0.18	0.11

Table 1: Weighted Pose Results: We compare Rotation Error, Translational Error, and Per-Point MSE for both training and validation objects.

## 5 Conclusions and Future Work

In conclusion, we have presented a method to combine the two architectures using weighted SVD. While this model is more of a proof-of-concept that attempts to unify the two architectures, it is worth pointing out that using the two models for the two categories of objects is able to help us generate goal poses for various free-floating and articulated objects. Moreover, by finetuning pretrained models from a weighted SVD combination, we are able to outperform the models on their respective training datasets categories. In future work, we wish to generalize the mathematics of the combined architecture beyond tasks that involve articulated and free-floating objects. We would also like to explore how such a unified architecture can aid motion planning as a geometric suggestor.

## References

- [1] Yahav Avigal, Samuel Paradis, and Harry Zhang. 6-dof grasp planning using fast 3d reconstruction and grasp quality cnn. *arXiv preprint arXiv:2009.08618*, 2020.
- [2] Yahav Avigal, Vishal Satish, Zachary Tam, Huang Huang, Harry Zhang, Michael Danielczuk, Jeffrey Ichnowski, and Ken Goldberg. Avplug: Approach vector planning for unicontact grasping amid clutter. In *2021 IEEE 17th International Conference on Automation Science and Engineering (CASE)*, pages 1140–1147. IEEE, 2021.
- [3] Dmitry Berenson, Siddhartha Srinivasa, and James Kuffner. Task space regions: A framework for pose-constrained manipulation planning. *The International Journal of Robotics Research*, 30(12):1435–1460, 2011.
- [4] Felix Burget, Armin Hornung, and Maren Bennewitz. Whole-body motion planning for manipulation of articulated objects. In *2013 IEEE International Conference on Robotics and Automation*, pages 1656–1662, May 2013.
- [5] Jae-Sook Cheong, A Frank Van Der Stappen, Ken Goldberg, Mark H Overmars, and Elon Rimon. Immobilizing Hinged Polygons. *Int. J. Comput. Geom. Appl.*, 17(01):45–69, February 2007.
- [6] Sachin Chitta, Benjamin Cohen, and Maxim Likhachev. Planning for autonomous door opening with a mobile manipulator. In *2010 IEEE International Conference on Robotics and Automation*, pages 1799–1806, May 2010.
- [7] Shivin Devgon, Jeffrey Ichnowski, Ashwin Balakrishna, Harry Zhang, and Ken Goldberg. Orienting novel 3d objects using self-supervised learning of rotation transforms. In *2020 IEEE 16th International Conference on Automation Science and Engineering (CASE)*, pages 1453–1460. IEEE, 2020.
- [8] Asher Elmquist, Aaron Young, Thomas Hansen, Sriram Ashokkumar, Stefan Caldararu, Abhiraj Dashora, Ishaan Mahajan, Harry Zhang, Luning Fang, He Shen, et al. Art/atk: A research platform for assessing and mitigating the sim-to-real gap in robotics and autonomous vehicle engineering. *arXiv preprint arXiv:2211.04886*, 2022.
- [9] Peter R Florence, Lucas Manuelli, and Russ Tedrake. Dense object nets: Learning dense visual object descriptors by and for robotic manipulation. In *Conference on Robot Learning*, pages 373–385. PMLR, 2018.

- [10] Yisheng He, Wei Sun, Haibin Huang, Jianran Liu, Haoqiang Fan, and Jian Sun. Pvn3d: A deep point-wise 3d keypoints voting network for 6dof pose estimation. In *Proceedings of the IEEE/CVF conference on computer vision and pattern recognition*, pages 11632–11641, 2020.
- [11] Yisheng He, Haibin Huang, Haoqiang Fan, Qifeng Chen, and Jian Sun. Ffb6d: A full flow bidirectional fusion network for 6d pose estimation. In *Proceedings of the IEEE/CVF Conference on Computer Vision and Pattern Recognition*, pages 3003–3013, 2021.
- [12] Ruizhen Hu, Wenchao Li, Oliver Van Kaick, Ariel Shamir, Hao Zhang, and Hui Huang. Learning to predict part mobility from a single static snapshot. *ACM Trans. Graph.*, 36(6):1–13, November 2017.
- [13] Ajinkya Jain, Rudolf Lioutikov, Caleb Chuck, and Scott Niekum. ScrewNet: Category-independent articulation model estimation from depth images using screw theory. In *2021 IEEE International Conference on Robotics and Automation (ICRA)*, pages 13670–13677, May 2021.
- [14] David Jin, Sushrut Karmalkar, Harry Zhang, and Luca Carlone. Multi-model 3d registration: Finding multiple moving objects in cluttered point clouds. *arXiv preprint arXiv:2402.10865*, 2024.
- [15] Dov Katz, Yuri Pyuro, and Oliver Brock. Learning to manipulate articulated objects in unstructured environments using a grounded relational representation. In *Robotics: Science and Systems IV*. Robotics: Science and Systems Foundation, June 2008.
- [16] Xiaolong Li, He Wang, Li Yi, Leonidas J Guibas, A Lynn Abbott, and Shuran Song. Category-Level articulated object pose estimation, 2020.
- [17] Vincent Lim, Huang Huang, Lawrence Yunliang Chen, Jonathan Wang, Jeffrey Ichnowski, Daniel Seita, Michael Laskey, and Ken Goldberg. Planar robot casting with real2sim2real self-supervised learning. *arXiv preprint arXiv:2111.04814*, 2021.
- [18] Vincent Lim, Huang Huang, Lawrence Yunliang Chen, Jonathan Wang, Jeffrey Ichnowski, Daniel Seita, Michael Laskey, and Ken Goldberg. Real2sim2real: Self-supervised learning of physical single-step dynamic actions for planar robot casting. In *2022 International Conference on Robotics and Automation (ICRA)*, pages 8282–8289. IEEE, 2022.
- [19] David G Lowe. Object recognition from local scale-invariant features. In *Proceedings of the seventh IEEE international conference on computer vision*, volume 2, pages 1150–1157. Ieee, 1999.
- [20] Lucas Manuelli, Wei Gao, Peter Florence, and Russ Tedrake. kpm: Keypoint affordances for category-level robotic manipulation. *International Symposium on Robotics Research (ISRR) 2019*, 2019.
- [21] Lucas Manuelli, Yunzhu Li, Pete Florence, and Russ Tedrake. Keypoints into the future: Self-supervised correspondence in model-based reinforcement learning. In *Conference on Robot Learning*, pages 693–710. PMLR, 2021.
- [22] Kaichun Mo, Shilin Zhu, Angel X Chang, Li Yi, Subarna Tripathi, Leonidas J Guibas, and Hao Su. Partnet: A large-scale benchmark for fine-grained and hierarchical part-level 3d object understanding. In *Proceedings of the IEEE/CVF Conference on Computer Vision and Pattern Recognition*, pages 909–918, 2019.
- [23] Kaichun Mo, Leonidas J Guibas, Mustafa Mukadam, Abhinav Gupta, and Shubham Tulsiani. Where2act: From pixels to actions for articulated 3d objects. In *Proceedings of the IEEE/CVF International Conference on Computer Vision*, pages 6813–6823, 2021.
- [24] Venkatraman Narayanan and Maxim Likhachev. Task-oriented planning for manipulating articulated mechanisms under model uncertainty. In *2015 IEEE International Conference on Robotics and Automation (ICRA)*, pages 3095–3101, May 2015.
- [25] Chuer Pan, Brian Okorn, Harry Zhang, Ben Eisner, and David Held. Tax-pose: Task-specific cross-pose estimation for robot manipulation. *arXiv preprint arXiv:2211.09325*, 2022.



- [26] Chuer Pan, Brian Okorn, Harry Zhang, Ben Eisner, and David Held. Tax-pose: Task-specific cross-pose estimation for robot manipulation. In *Conference on Robot Learning*, pages 1783–1792. PMLR, 2023.
- [27] Zengyi Qin, Kuan Fang, Yuke Zhu, Li Fei-Fei, and Silvio Savarese. Keto: Learning keypoint representations for tool manipulation. In *2020 IEEE International Conference on Robotics and Automation (ICRA)*, pages 7278–7285. IEEE, 2020.
- [28] Fred Rothganger, Svetlana Lazebnik, Cordelia Schmid, and Jean Ponce. 3d object modeling and recognition using local affine-invariant image descriptors and multi-view spatial constraints. *International journal of computer vision*, 66(3):231–259, 2006.
- [29] Sitian Shen, Zilin Zhu, Linqian Fan, Harry Zhang, and Xinxiao Wu. Diffclip: Leveraging stable diffusion for language grounded 3d classification. In *Proceedings of the IEEE/CVF Winter Conference on Applications of Computer Vision*, pages 3596–3605, 2024.
- [30] Khe Chai Sim, Françoise Beaufays, Arnaud Benard, Dhruv Guliani, Andreas Kabel, Nikhil Khare, Tamar Lucassen, Petr Zadrazil, Harry Zhang, Leif Johnson, et al. Personalization of end-to-end speech recognition on mobile devices for named entities. In *2019 IEEE Automatic Speech Recognition and Understanding Workshop (ASRU)*, pages 23–30. IEEE, 2019.
- [31] Anthony Simeonov, Yilun Du, Andrea Tagliasacchi, Joshua B Tenenbaum, Alberto Rodriguez, Pulkit Agrawal, and Vincent Sitzmann. Neural descriptor fields: Se (3)-equivariant object representations for manipulation. In *2022 International Conference on Robotics and Automation (ICRA)*, pages 6394–6400. IEEE, 2022.
- [32] Dylan Turpin, Liquan Wang, Stavros Tsogkas, Sven Dickinson, and Animesh Garg. Gift: Generalizable interaction-aware functional tool affordances without labels. *Robotics: Science and Systems (RSS)*, 2021.
- [33] Mel Vecerik, Jean-Baptiste Regli, Oleg Sushkov, David Barker, Rugile Pevceviciute, Thomas Rothörl, Raia Hadsell, Lourdes Agapito, and Jonathan Scholz. S3k: Self-supervised semantic keypoints for robotic manipulation via multi-view consistency. In *Conference on Robot Learning*, pages 449–460. PMLR, 2021.
- [34] Xiaogang Wang, Bin Zhou, Yahao Shi, Xiaowu Chen, Qinqing Zhao, and Kai Xu. Shape2motion: Joint analysis of motion parts and attributes from 3d shapes. In *Proceedings of the IEEE/CVF Conference on Computer Vision and Pattern Recognition*, pages 8876–8884, 2019.
- [35] Fanbo Xiang, Yuzhe Qin, Kaichun Mo, Yikuan Xia, Hao Zhu, Fangchen Liu, Minghua Liu, Hanxiao Jiang, Yifu Yuan, He Wang, and Others. Sapien: A simulated part-based interactive environment. In *Proceedings of the IEEE/CVF Conference on Computer Vision and Pattern Recognition*, pages 11097–11107, 2020.
- [36] Yu Xiang, Tanner Schmidt, Venkatraman Narayanan, and Dieter Fox. Posecnn: A convolutional neural network for 6d object pose estimation in cluttered scenes. *Robotics: Science and Systems (RSS)*, 2018.
- [37] Zhenjia Xu, He Zhanpeng, and Shuran Song. Umpnet: Universal manipulation policy network for articulated objects. *IEEE Robotics and Automation Letters*, 2022.
- [38] Zihao Yan, Ruizhen Hu, Xingguang Yan, Luanmin Chen, Oliver Van Kaick, Hao Zhang, and Hui Huang. Rpm-net: recurrent prediction of motion and parts from point cloud. *arXiv preprint arXiv:2006.14865*, 2020.
- [39] Yupu Yao, Shangqi Deng, Zihan Cao, Harry Zhang, and Liang-Jian Deng. Apla: Additional perturbation for latent noise with adversarial training enables consistency. *arXiv preprint arXiv:2308.12605*, 2023.
- [40] Andy Zeng, Pete Florence, Jonathan Tompson, Stefan Welker, Jonathan Chien, Maria Attarian, Travis Armstrong, Ivan Krasin, Dan Duong, Vikas Sindhwani, et al. Transporter networks: Rearranging the visual world for robotic manipulation. In *Conference on Robot Learning*, pages 726–747. PMLR, 2021.

- [41] Vicky Zeng, Timothy E Lee, Jacky Liang, and Oliver Kroemer. Visual identification of articulated object parts. In *2021 IEEE/RSJ International Conference on Intelligent Robots and Systems (IROS)*, pages 2443–2450. IEEE, 2020.
- [42] Haolun Zhang. Health diagnosis based on analysis of data captured by wearable technology devices. *International Journal of Advanced Science and Technology*, 95:89–96, 2016.
- [43] Harry Zhang, Jeffrey Ichnowski, Yahav Avigal, Joseph Gonzales, Ion Stoica, and Ken Goldberg. Dex-net ar: Distributed deep grasp planning using a commodity cellphone and augmented reality app. In *2020 IEEE International Conference on Robotics and Automation (ICRA)*, pages 552–558. IEEE, 2020.
- [44] Harry Zhang, Jeffrey Ichnowski, Daniel Seita, Jonathan Wang, Huang Huang, and Ken Goldberg. Robots of the lost arc: Self-supervised learning to dynamically manipulate fixed-endpoint cables. In *2021 IEEE International Conference on Robotics and Automation (ICRA)*, pages 4560–4567. IEEE, 2021.
- [45] Harry Zhang, Ben Eisner, and David Held. Flowbot++: Learning generalized articulated objects manipulation via articulation projection. *arXiv preprint arXiv:2306.12893*, 2023.